Rosiglitazone remodels the lipid droplet and britens human visceral and subcutaneous adipocytes ex vivo[s]

Mi-Jeong Lee,[1,*,†] **Sukanta Jash,**[†,§] **Jessica E. C. Jones,**[**] **Vishwajeet Puri,**[†,§] **and Susan K. Fried**[*,†]

Diabetes, Obesity, and Metabolism Institute,* Icahn School of Medicine at Mount Sinai, New York, NY; Obesity Center,[†] Department of Medicine, and Department of Biochemistry,** Boston University School of Medicine, Boston, MA; and Department of Biomedical Sciences and Diabetes Institute,[§] Heritage College of Osteopathic Medicine, Ohio University, Athens, OH

ORCID ID: 0000-0002-8171-7913 (M-J.L.)

Abstract Treatment with PPARγ agonists in vivo improves human adipocyte metabolism, but the cellular mechanisms and possible depot differences in responsiveness to their effects are poorly understood. To examine the ex vivo metabolic effects of rosiglitazone (Rosi), we cultured explants of human visceral (omental) and abdominal subcutaneous adipose tissues for 7 days. Rosi increased mRNA levels of transcriptional regulators of brite/beige adipocytes (PGC1α, PRDM16), triglyceride synthesis (GPAT3, DGAT1), and lipolysis (ATGL) similarly in adipose tissues from both depots. In parallel, Rosi increased key modulators of FA oxidation (UCP1, FABP3, PLIN5 protein), rates of FA oxidation, and protein levels of electron transport complexes, suggesting an enhanced respiratory capacity as confirmed in newly differentiated adipocytes. Rosi led to the formation of small lipid droplets (SLDs) around the adipocyte central lipid droplet; each SLD was decorated with redistributed mitochondria that colocalized with PLIN5. SLD maintenance required lipolysis and FA reesterification. Rosi thus coordinated a structural and metabolic remodeling in adipocytes from both visceral and subcutaneous depots that enhanced oxidative capacity.[jlr] Selective targeting of these cellular mechanisms to improve adipocyte FA handling may provide a new approach to treat metabolic complications of obesity and diabetes.—Lee, M-J., S. Jash, J. E. C. Jones, V. Puri, and S. K. Fried. **Rosiglitazone remodels the lipid droplet and britens human visceral and subcutaneous adipocytes ex vivo.** *J. Lipid Res.* 2019. **60:** 856–868.

Supplementary key words thiazolidinedione • perilipins • fatty acid oxidation • adipose depots • protein carbonylation

White adipocytes are specialized cells that have a very high capacity to esterify and store FAs as triglyceride (TAG) within a single lipid droplet (LD) and release them as required by variations in nutritional state (1). In obesity, the adipocyte must cope with an increased flux of FAs from the diet and higher basal lipolysis (2, 3). If these FAs are not efficiently esterified or oxidized, unbound FAs within the cell cause lipotoxic stress with deleterious consequences for adipocyte metabolic and endocrine function (4–6). As the storage capacity of the adipocyte is exceeded in obesity, the overflow of FAs can lead to ectopic fat deposition and systemic metabolic dysfunction (1, 7, 8). Strategies to modify the metabolism of FAs in adipocytes have therapeutic potential in obesity-related metabolic diseases.

In contrast to multilocular brown or "brite"/beige adipocytes that are densely packed with mitochondria and express UCP1, white adipocytes contain relatively few mitochondria, low FA oxidation capacity, and much lower levels of UCP1 (9). White adipose tissue (WAT), however, can acquire brown-like features in response to β-adrenergic stimulation or cold. Studies in rodents have shown that brite/beige adipocytes can be formed from mature white adipocytes (10, 11) or the recruitment and differentiation of beige progenitors (12, 13). Several lines of evidence indicate that mature white human adipocytes can be metabolically reprogrammed to a more oxidative phenotype in

vivo. Chronic adrenergic stimulation in humans with pheochromocytoma (14) and severe burn injury (15) or direct cold exposure for several hours (16) induces remodeling of white to brite adipocytes. Treatment of obese or type 2 diabetes patients with rosiglitazone (Rosi) or pioglitazone also induces a more oxidative phenotype in subcutaneous adipose tissue, including higher rates of FA oxidation and increased expression levels of FA metabolic genes (7, 17) and UCP1 (18). Further, direct activation of PPARγ with thiazolidinediones drives a brite metabolic program in human adipocyte culture models (19–21), but we know of no studies that examined Rosi's effects on a brite metabolic program in mature human adipocytes ex vivo.

Significant remodeling of cellular components, including LDs and mitochondria, occurs during conversion from white to brite adipocytes. In humans, brite adipocytes induced by chronic exposure to catecholamines in vivo exhibit a mixture of paucilocular and multilocular LDs (14, 15). In early studies of ob/ob mice treated with Rosi, Corvera's group observed "small, droplet-like structures" surrounded by dense mitochondrial staining in adipocytes (22). In the course of carrying out studies of Rosi's actions on human adipocytes, we observed similar structural remodeling. We therefore went on to investigate the biochemical mechanisms that led to the formation of small LDs (SLDs) and their interaction with mitochondria in human adipocytes.

Perilipins are LD proteins that are expressed in a cell-specific manner and play active roles in the regulation of lipolysis, FA oxidation, and (re)esterification of FAs (23). In white adipocytes, PLIN1 is the major LD protein (24), while more oxidative tissues, including skeletal muscle and brown adipose tissue (BAT), selectively express PLIN5 (25–27). Both PLIN1 and PLIN5 limit basal lipolysis but facilitate stimulated lipolysis (23). However, PLIN5 differs from PLIN1 in that it physically interacts with mitochondria and may direct FAs to the mitochondria for β-oxidation (25–27). Treatment with PPARγ agonists increases PLIN5 expression in WAT of mice in vivo (25) and in human multipotent adipose-derived stem cells (hMADs) in vitro (21), so we studied how Rosi affected its expression and cellular localization in mature human adipocytes.

Adipose tissues from different anatomical fat depots may have different capacities to acquire brown-like phenotypes. In mice, subcutaneous (inguinal) adipose tissues brown or "briten" after cold exposure, β-adrenergic receptor stimulation, or PPARγ agonist treatment, but most studies do not show browning of the "visceral" (epididymal) depot of male rodents (28–31). In humans, brown-like phenotypes were found in both visceral omental (Om) (14) and subcutaneous adipose tissues after chronic adrenergic activation (15), but another study detected UCP1-positive adipocytes only in the periadrenal fat (32). In the current study, we considered the possibility that human white adipocytes from both visceral and subcutaneous depots could be reprogrammed by activation of PPARγ to increase their metabolic and respiratory capacity. We used an organ culture system that maintains expression of key adipocyte genes over 7 days ex vivo in a 3D context and a physiologically relevant hormone milieu (insulin and glucocorticoid as

modeled by dexamethasone) (33). Collectively, our results reveal that white human adipocytes from both visceral and subcutaneous depots can be metabolically reprogrammed toward a more oxidative phenotype.

MATERIALS AND METHODS

Human subjects

Om adipose tissues and abdominal subcutaneous adipose tissues (ASATs) were obtained during elective surgeries from a total of 39 subjects [BMI, 40.5 ± 1.6 kg/m^2 (range 23–63 kg/m^2); age, 41.4 ± 2.0 years (range 25–71 years)] who were free of diabetes, cancers, and endocrine or inflammatory diseases by medical history. Surgeries took place at the Boston Medical Center. All subjects provided informed consent as approved by the Institutional Review Boards of the Boston Medical Center and all studies abided by the Declaration of Helsinki principles. Subject characteristics are provided in supplemental Table S1. All experiments were repeated on samples from at least three different donors. The number of subjects that were used for each experiment is provided in the figure legends.

Adipose tissue processing and organ culture

Adipose tissues were placed in room temperature medium 199 (Life Technologies), transferred to the laboratory, minced into small fragments ($\sim$5–10 mg), and placed in organ culture with insulin (0.7 nM) and dexamethasone (10 nM) without or with Rosi (1 μM) for up to 7 days in serum-free medium 199, as previously described (33). Aliquots of media from the final day of culture were frozen at $-80°$C for glycerol measurements. After culture, tissues were used for isolation of fat cells and stromal vascular cells by collagenase digestion (1 mg/ml type 1; Worthington Biochemical) (33) or quick frozen in liquid nitrogen and used for immunoblotting, RNA expression, or isolation of mitochondria. To assess the importance of lipolysis and reesterification, orlistat (100 μM) or triacsin C (2 μM) was added during the final 2 days of culture after 5 days of treatment with or without Rosi.

RNA extraction and RT-qPCR

Total RNA was extracted using Trizol (Thermo-Fisher) and RNA quantity and quality were assessed spectrophotometrically (Nano-Drop; Thermo-Fisher). After reverse transcription (Transcriptor First Strand cDNA synthesis kit; Roche), quantitative (q)PCR was performed using TaqMan probes (Thermo-Fisher) and a Light Cycler 480 II (Roche). Expression levels relative to cyclophilin A are presented.

Transcriptome

Human Gene 1.0 ST microarrays (Affymetrix) were used to profile gene expression patterns in the control and Rosi-treated Om adipose tissues from two obese women (33 years old, Hispanic, BMI = 43.0 kg/m^2; 62 years old, Caucasian, BMI = 31.4 kg/m^2). Microarray analysis was performed by the Microarray Resource Core of the Clinical and Translational Science Institute of Boston University and deposited in NCBI's Gene Expression Omnibus (GSE122721). The arrays were normalized using the Robust Multi-array Average algorithm and a Chip definition file that maps the probes on the array to unique Entrez Gene identifiers. Technical duplicates of the first subject were averaged with the values from the second subject prior to statistical analysis. A linear mixed-effects model was used to identify genes that changed after Rosi treatment while adjusting for inter-donor variability. The transcripts significantly up- or down-regulated by Rosi (FDR

q < 0.05) were used for functional enrichment analysis with DAVID (https://david.ncifcrf.gov/) (33). Significantly enriched ($P < 0.01$) KEGG pathways are reported.

Western blotting

Tissues and cells were homogenized in lysis buffer (Cell Signaling) supplemented with 10% SDS (to assure extraction of LD proteins) and protease inhibitor cocktail, and processed (34). Proteins were resolved in 10% NuPAGE Bis-Tris gels in MOPS-SDS or MES-SDS running buffer and transferred to PVDF membranes (Thermo-Fisher). After blocking in 5% milk, proteins were blotted for UCP1 (ab10983; Abcam), porin (ab15895; Abcam), PLIN5 (GP31; Progen Biotechnik), FABP3 (gift from Dr. Judith Storch, Rutgers University), ATGL (34), electron transport chain (ETC) proteins (ab110411; Abcam), and HSP90 (sc-7947; Santa Cruz Biotechnology) followed by incubation with appropriate secondary antibodies conjugated with HRP and capture of chemiluminescence images.

Isolation of mitochondria and measurement of ETC complex proteins

Mitochondria were isolated from frozen adipose tissues following previously described procedures (35) with slight modifications. Briefly, tissue was homogenized in mitochondrial isolation buffer (0.3 M sucrose, 10 mM HEPES, 1 mM EGTA) supplemented with 1% BSA followed by centrifugation steps at 500 g for 10 min, at 700 g for 10 min, and finally at 7,000 g for 10 min. The final pellet was resuspended in the mitochondrial isolation buffer, and protein was quantified using the BCA protein assay kit (Thermo-Fisher) and used for immunoblotting of ETC proteins.

FA oxidation

Adipose tissues (total of ~100 mg) that had been cultured under specified conditions were incubated with ^{14}C-oleic acid (1 μCi/ml) in 1 ml Krebs-Ringer bicarbonate (KRB) buffer with 0.2 mM oleic acid, 5 mM glucose, and 4% BSA under an atmosphere of 95% O_2:5% CO_2 for 3 h. Complete oxidation of ^{14}C-oleate to $^{14}CO_2$ was measured (21).

Lipolysis

Lipolysis during culture was measured by glycerol accumulation during the final day of culture. Glycerol concentrations were determined fluorometrically (36) and normalized to tissue weight. To more directly assess changes in lipolytic capacity, we also performed acute incubations of isolated adipocytes from Om tissues treated with or without Rosi. Incubations were carried out in KRB buffer with 5 mM glucose and 4% BSA (pH 7.4) for 2 h in the basal or stimulated conditions with atrial natriuretic peptide (ANP; 2 or 10 nM), norepinephrine (10^{-6} M), or isoproterenol (Iso; 10^{-6} M), as previously described (37). Glycerol release data were normalized to adipocyte lipid weight after Dole's extraction (37).

Measurement of cardiolipin mass

Lipid extraction and MS-based detection of cardiolipin were performed through Michigan Nutrition and Obesity Research Center. The lipids were extracted from adipose tissues using a modified Bligh-Dyer method, extraction with 2:2:2 (v/v/v) water/methanol/dichloromethane. After spiking internal standards, the organic layer was collected and dried under a stream of nitrogen. The dried extract was resuspended and injected into a Waters Acquity HSS T3 column in a LC-MS system (Waters). Cardiolipin content was quantified and normalized to tissue weight.

Confocal imaging of mitochondria and LDs

Isolated adipocytes from freshly obtained adipose tissues and after culture were used for staining of mitochondria and lipid. Adipocytes were incubated with MitoTracker-Green, MitoTracker-Red, or LipidTOX-Deep Red (Thermo-Fisher) for 1 h. After washing, live cells were mounted on slides with DAPI mounting media (Vector Labs) and confocal microscopy was performed using a Zeiss LSM 710-Live Duo scan (Carl Zeiss, Germany) or Nikon A1Rsi confocal microscope (Tokyo, Japan) with a 100× oil immersion objective. Images were processed using Metamorph imaging software (Universal Imaging).

Immunocytochemistry of PLIN1 and PLIN5 and fluorescence microscopy

Isolated control or brite adipocytes were stained with mitochondria (MitoTracker-Red) and neutral lipid (LipidTOX-Deep Red) for 1 h and fixed in 4% paraformaldehyde for 20 min. After permeabilization in 0.1% Triton X-100 for 5 min and blocking in 2% BSA for 1 h, cells were incubated with rabbit anti-human PLIN1 and guinea pig anti-human PLIN5 (GP31; Progen Biotechnik) antibodies for 2 h, followed by incubation with goat anti-rabbit IgG Alexa Flour 488 and goat anti-guinea pig IgG Alexa Flour 488 antibodies (Thermo-Fisher), respectively, for 1 h. Cells were mounted with DAPI mounting media and fluorescence imaging was performed using a Nikon A1Rsi confocal microscope.

Primary culture of newly differentiated human adipocytes

Adipose tissue stromal cells were isolated by collagenase digestion of ASAT, cultured, and differentiated following our published protocol (38). Fully differentiated adipocytes (day 14) were treated with Rosi (1 μM) for up to 7 days in maintenance media with refeeding every 2 days and 1 day prior to final assays.

Oxygen consumption measurement in primary cultures of newly differentiated human adipocytes

Cells were seeded, grown, and differentiated in XF24 V7 plates (Seahorse Bioscience). After treating differentiated adipocytes with or without Rosi for 7 days, oxygen consumption rates (OCRs) were measured using an XF24 analyzer (Seahorse Bioscience). Two hours prior to OCR measurement, the medium was replaced with Seahorse XF assay medium (102365-100; Seahorse Bioscience) and incubated at 37°C for 60 min. Four assay cycles of 1 min mix, 3 min wait, and 3 min measurement were used to determine basal respiration. ATP-linked (coupled) respiration was inhibited by oligomycin (5 μM), and maximum respiratory capacity was assessed after addition of carbonyl cyanide-p-trifluoromethoxy-phenylhydrazone (FCCP; 1 mM). Finally, mitochondrial respiration was blocked by an equal mixture of rotenone (an inhibitor of complex I) and antimycin A (an inhibitor of complex III), 5 μm each. Only FCCP was injected together with Na-pyruvate (10 mM). Basal, maximal, ATP-linked, and proton-leak (uncoupled with ATP synthesis) OCRs, coupling efficiencies, and cell respiratory control ratios were calculated (39).

Protein oxidation assay

Protein carbonylation was measured with an OxyBlot protein oxidation detection kit (Millipore) following the manufacturer's instructions. Total carbonylation was visualized by chemiluminescence and quantified.

Statistics

Data are presented as the mean ± SEM of the number of independent experiments as indicated. One- or two-way ANOVA was used to test the Rosi effects and interactions of Rosi and depot,

followed by post hoc Student paired *t*-tests when the main effects or interactions were significant using GraphPad 5.0 software. Differences between means were considered statistically different when $P < 0.05$.

RESULTS

Rosi induced a more oxidative phenotype in both human Om and ASAT

To address potential depot differences in response to Rosi, we compared its effects between visceral Om and ASAT. Rosi markedly increased expression of transcripts known to be enriched in brown and beige adipocytes, including the transcriptional regulators, *PGC1α, PRDM16*, and *CITED1* (12, 40), similarly in both depots (**Fig. 1A**). Rosi also induced expression of mRNA and proteins involved in FA metabolism in BAT, including UCP1, PLIN5, and FABP3 (25, 41), in both Om and ASAT (Fig. 1A, B). The changes in mRNA and protein levels of UCP1 and PLIN5 were observed in mature adipocytes, not stromal cells (Fig. 1C and D). FABP3 was induced in both adipocytes and stromal cells. Upregulation of these genes could be detected after 2 days of Rosi treatment (data not shown).

Rosi modified FA handling: increased lipolysis during culture and FA oxidation in both Om and ASAT

Lipolysis. Rosi significantly increased lipolysis during the final day of culture as measured by glycerol accumulation in the media by $32.3 \pm 8.9\%$ in Om adipose tissue and
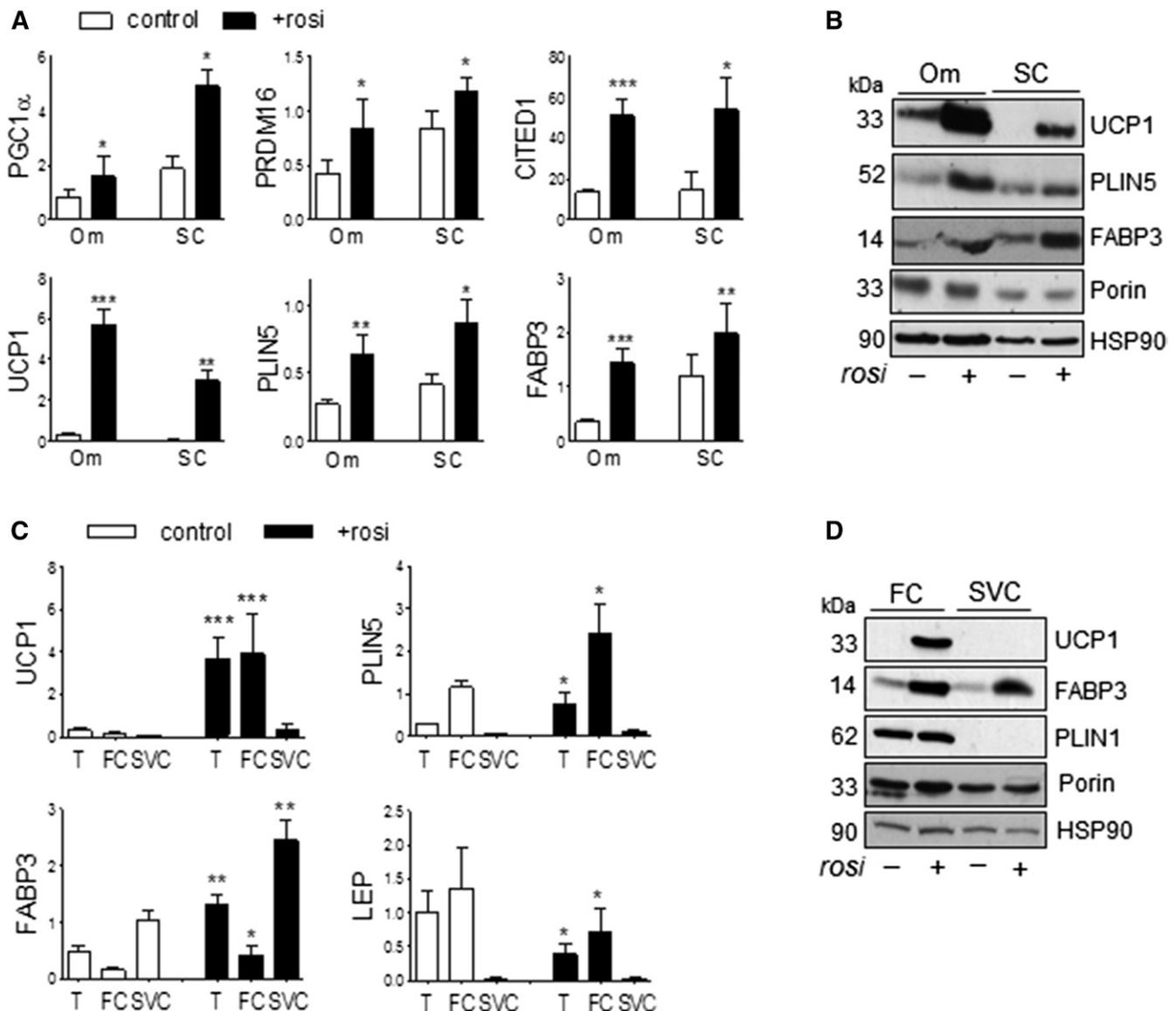
Fig. 1. Rosi induced brite phenotypes in both Om adipose tissues and subcutaneous human adipose tissues. A, B: mRNA and protein levels of genes known to be more abundantly expressed in brown and brite than white adipocytes were measured in Om adipose tissues and abdominal subcutaneous (SC) human adipose tissues that had been cultured without or with Rosi (1 μM) for 7 days. C, D: After treating Om adipose tissue without or with Rosi, fat cells (FC) and stromal vascular cells (SVC) were isolated with collagenase digestion and mRNA and protein levels were measured in tissue (T), FCs, and SVCs. Data are expressed as the mean ± SEM of five to nine experiments [BMI, 37.5 ± 3.7 kg/m^2 (range 29–54 kg/m^2); age, 50.8 ± 4.0 years (range 36–71 years); seven female/two male]. *$P < 0.05$, **$P < 0.01$, ***$P < 0.001$ (paired *t*-tests after one- or two-way ANOVA).

35.4 ± 10.2% in ASAT (**Fig. 2A**). To assess how Rosi regulated rates of basal and stimulated lipolysis under defined conditions, we isolated adipocytes from Om adipose tissues cultured with or without Rosi for 7 days and incubated them for 2 h in KRB buffer with a FA acceptor, BSA. Culture with Rosi decreased rates of basal lipolysis but did not affect rates of ANP-, norepinephrine-, or Iso-stimulated lipolysis (Fig. 2B). Because of the lower basal lipolytic rates, the fold induction by the stimuli was greater in adipocytes isolated from Rosi-treated tissues, e.g., Iso: 1.8-fold versus 2.3-fold in control and Rosi-treated conditions, respectively ($P < 0.01$, n = 7).

FA oxidation. Culture with Rosi enhanced rates of FA oxidation as assessed by the complete oxidation of ^{14}C-oleate into $^{14}CO_2$ by 95 ± 15% in Om adipose tissue and 65 ± 8% in ASAT (Fig. 2C). Rosi increased protein levels of mitochondrial respiratory chain subunits in both depots (Fig. 2D), suggesting higher mitochondrial oxidative capacity.

Rosi modulated the expression of multiple transcripts involved in FA turnover, mitochondrial oxidative capacity, inflammation, and endocrine function similarly in Om and ASAT

Because Rosi increased mRNA levels of *PGC1α* and *UCP1* similarly in Om and ASAT, we examined expression of other genes typical of brite adipocytes, focusing on FA metabolism, mitochondrial oxidation, and adipokines. Rosi increased mRNA levels of *ATGL*, the rate-determining TAG lipase, without affecting *HSL* and *PLIN1* in both depots (**Fig. 3A**). Rosi increased expression of key genes in mitochondrial FA uptake and oxidation (*CPT1A*, *CTP1B*, *ACADM*), oxidative phosphorylation (*SDHB*, *NDUFB5*), and ATP synthesis (*ATP5B*) as well as genes in cellular uptake of TAG-FA (*LPL*, *CD36*) and esterification (*GPAT3*, *DGAT1*) (Fig. 3B). Expression of transcripts needed for the synthesis of the glyceride-glycerol backbone of TAG, the insulin sensitive glucose transporter (*GLUT4*) and the glyceroneogenic enzyme (*PCK1*), were both increased, as were

ACC1 and *FAS*, the rate-determining steps of de novo FA synthesis.

As expected, Rosi decreased expression of adipokines (*LEP*, *SAA1*) and proinflammatory cytokines (*IL-6*, *TNF*), while increasing *ADIPOQ*, an anti-inflammatory and insulin-sensitizing adipokine, in both depots (Fig. 3C).

Rosi remodeled adipocyte mitochondria and LDs

Rosi had only a modest effect on mitochondrial mass, as judged by the 20 ± 6% increases in protein levels of porin ($P < 0.05$, n = 5) (Fig. 1D), yet more substantially increased oxidative capacity, as indicated by the induction of FA oxidation rates and protein levels of ETC complexes (Fig. 2C, D). In addition, Rosi increased cardiolipin, a mitochondrial phospholipid (42), in Om adipose tissue (control; 11.0 ± 1.8 nmol/mg tissue vs. 15.1 ± 1.4 nmol/mg tissue, $P < 0.05$, n = 4) as well as the mRNA level of *CRLS1* in both Om and ASAT (Fig. 3B, last panel).

We next used confocal microscopy to study the structural organization of mitochondria and LDs in adipocytes isolated from control and Rosi-treated Om tissues, as greater amounts of these tissues were routinely available. Control white adipocytes had a large single LD (50–150 μm) that occupied most of the cell volume, and mitochondria were evenly distributed on its surface (**Fig. 4A**, B; top panels). In controls, subject-dependent variations in mitochondrial morphology were observed, showing punctate to more elongated ribbon-like structures that indicate mitochondrial networking. The variations in mitochondrial morphology among cells from the control condition were very similar to those in freshly obtained adipocytes isolated immediately after surgical excision of tissue (data not shown).

Culture with Rosi led to appearance of clusters of SLDs (1–2 μm) on the surface of the main central LD that was ~100 μm in diameter (Fig. 4A, B; middle and bottom panels). Furthermore, most mitochondria were rearranged such that they surrounded SLDs. In Rosi-treated cells, mitochondria were more punctate and, in contrast to controls, no elongated ribbon-like structures were observed.
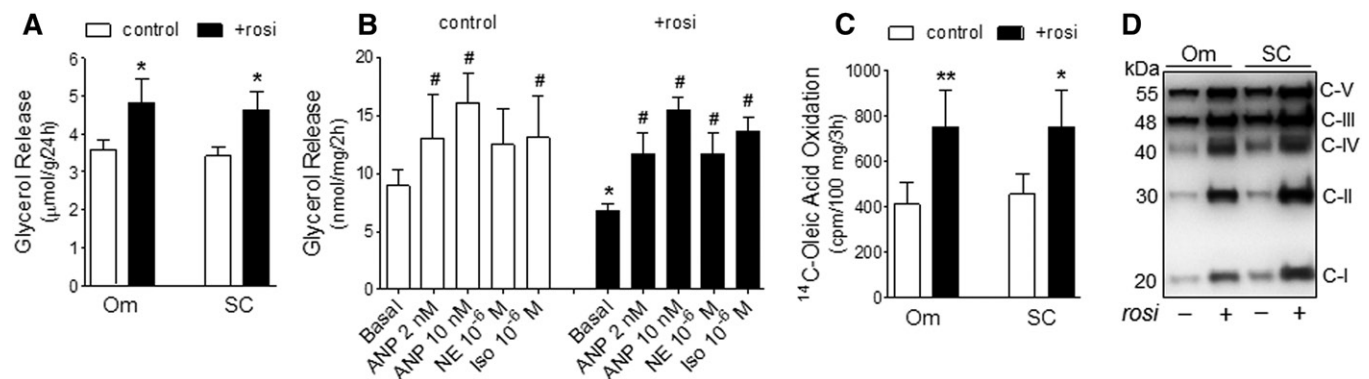
Fig. 2. Effects of Rosi on lipolytic rates and FA oxidative capacity in human adipocytes. A: Glycerol accumulation in culture media during the final 24 h. *$P < 0.05$ with paired *t*-tests after two-way ANOVA, n = 6. B: Lipolytic capacity under basal and stimulated conditions was measured in isolated adipocytes from control or Rosi-treated Om tissues. Data are expressed as the mean ± SEM of seven experiments. *$P < 0.05$ (control vs. Rosi); #$P < 0.05$ compared with the basal within each condition (post hoc paired *t*-tests) after RM-ANOVA (F = 3.22, $P = 0.004$). C: FA oxidation rates (^{14}C-oleate oxidation to $^{14}CO_2$) in adipose tissues cultured with or without Rosi. Data are expressed as the mean ± SEM of four experiments. *$P < 0.05$, **$P < 0.01$ with paired *t*-tests. D: Expression levels of mitochondrial ETC proteins were measured in isolated mitochondria after 7 days of treatment with Rosi and a representative Western blot of three (Om) or four subcutaneous (SC) are shown.

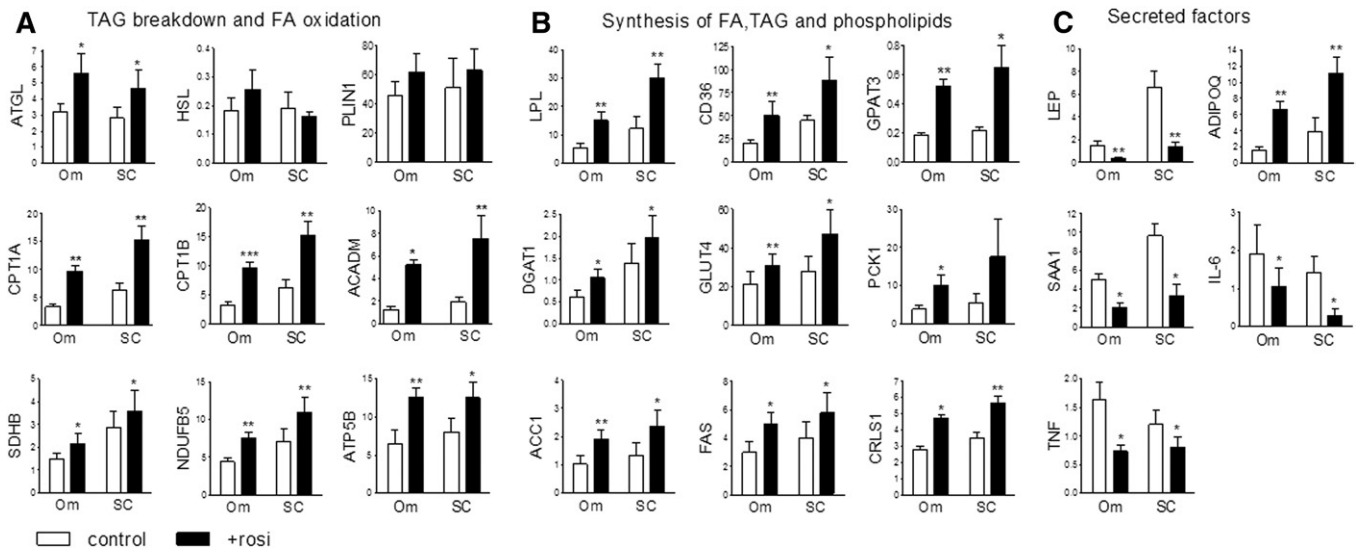**Fig. 3.** Rosi increased expression levels of genes involved in TAG turnover while suppressing inflammatory markers in both Om adipose tissues and subcutaneous human adipose tissues. Expression levels of mRNAs in TAG breakdown and FA oxidation (A), synthesis of FA, TAG, and phospholipids (B), and secretory factors (C) were measured in control or Rosi-treated Om and abdominal subcutaneous (SC) adipose tissues with qPCR. Data are expressed as the mean ± SEM of values from five to nine subjects [BMI, 37.5 ± 3.7 kg/m^2 (range 29–54 kg/m^2); age, 50.8 ± 4.0 years (range 36–71 years); seven female/two male]. $*P < 0.05$, $**P < 0.01$, $***P < 0.001$ (paired t-tests after two-way ANOVA).

The 3D volume view (last panel in Fig. 4B) confirmed that this reorganization occurred near the surface of the large LD and not in its core. Time course experiments showed that the reorganization started as early as 1 day after Rosi treatment and increased over time; about 30–40% of the adipocytes exhibited the remodeled phenotype on day 2, and most of the adipocytes showed remodeling after 7 days ($87 \pm 4\%$, n = 5 cultures from different subjects), indicating that it is a progressive process. A similar remodeling was observed in ASAT (supplemental Fig. S1).

Mechanism of SLD formation: inhibition of lipolysis or FA activation blocked the formation of SLDs

SLDs could be formed via fragmentation of the main droplet or reesterification of FAs released by lipolysis. To understand the mechanism by which SLDs were formed,

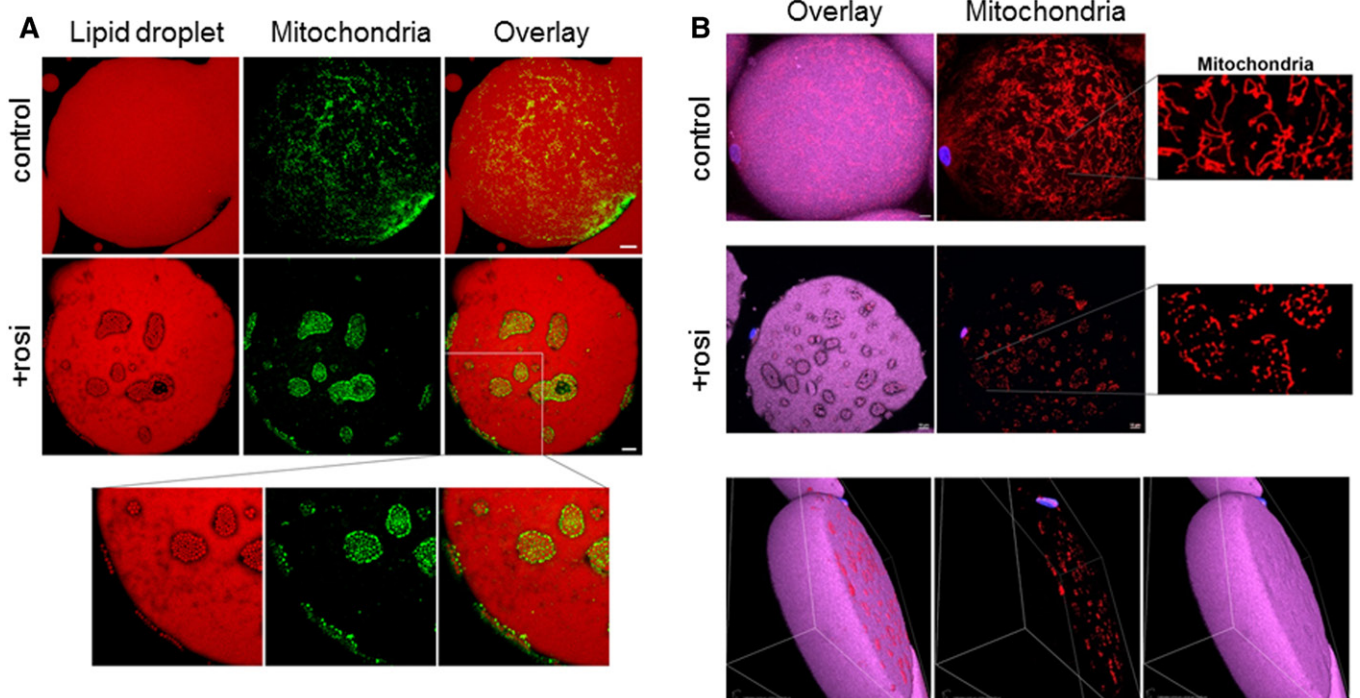**Fig. 4.** Rosi induced remodeling of LDs and rearrangement of mitochondria in human adipocytes. Isolated adipocytes from control or Rosi-treated Om tissues were used for confocal imaging of LDs and mitochondria. Neutral lipids were labeled with LipidTOX-Deep Red, mitochondria were stained with Mitotracker-Green (A) or Mitotracker-Red (B), and nuclei were stained with DAPI. White scale bars = 10 μm.

Om tissues were treated with Rosi for 7 days with orlistat (an inhibitor of lipases) or triacsin C (an inhibitor of FA activation by ACSLs) added during the final 2 days of culture. In control adipocytes, triacsin C or orlistat did not affect LD or mitochondrial morphology (data not shown). Triacsin C blocked the Rosi-mediated formation of SLDs, and mitochondria remained uniformly distributed, as in the control cells (**Fig. 5**). Inhibition of lipolysis with orlistat in Rosi-treated adipocytes also led to disappearance of apparent SLDs, but not the mitochondrial rearrangement (Fig. 5).

Rosi increased expression of PLIN5 that decorated SLDs and colocalized with mitochondria

As we found that most of the mitochondria were surrounding the clusters of SLDs, not the central droplet, and PLIN5 was induced in brite adipocytes, we evaluated whether the PLIN coating of the large and small droplets

differed. Adipocytes, isolated from control or Rosi-treated tissues, were stained for lipid and mitochondria followed by immunodetection of PLIN1 or PLIN5. As expected (43), the unilocular LD in control adipocytes was coated with PLIN1 and no significant PLIN5 staining was detected (data not shown). In Rosi-treated adipocytes, the large central droplet was coated with PLIN1 but not PLIN5, while the SLDs were decorated with both PLIN1 and PLIN5 (**Fig. 6A**, B). Confocal imaging showed that PLIN5 compared with PLIN1 was more closely associated with mitochondria on the small droplets.

Rosi acted directly on adipocytes to increase respiratory capacity

Multiple cell types are present within adipose tissues, so it is not possible to determine whether the effects of Rosi on the adipocytes are direct or mediated by other cells types. Similarly, measurements of oxygen consumption in
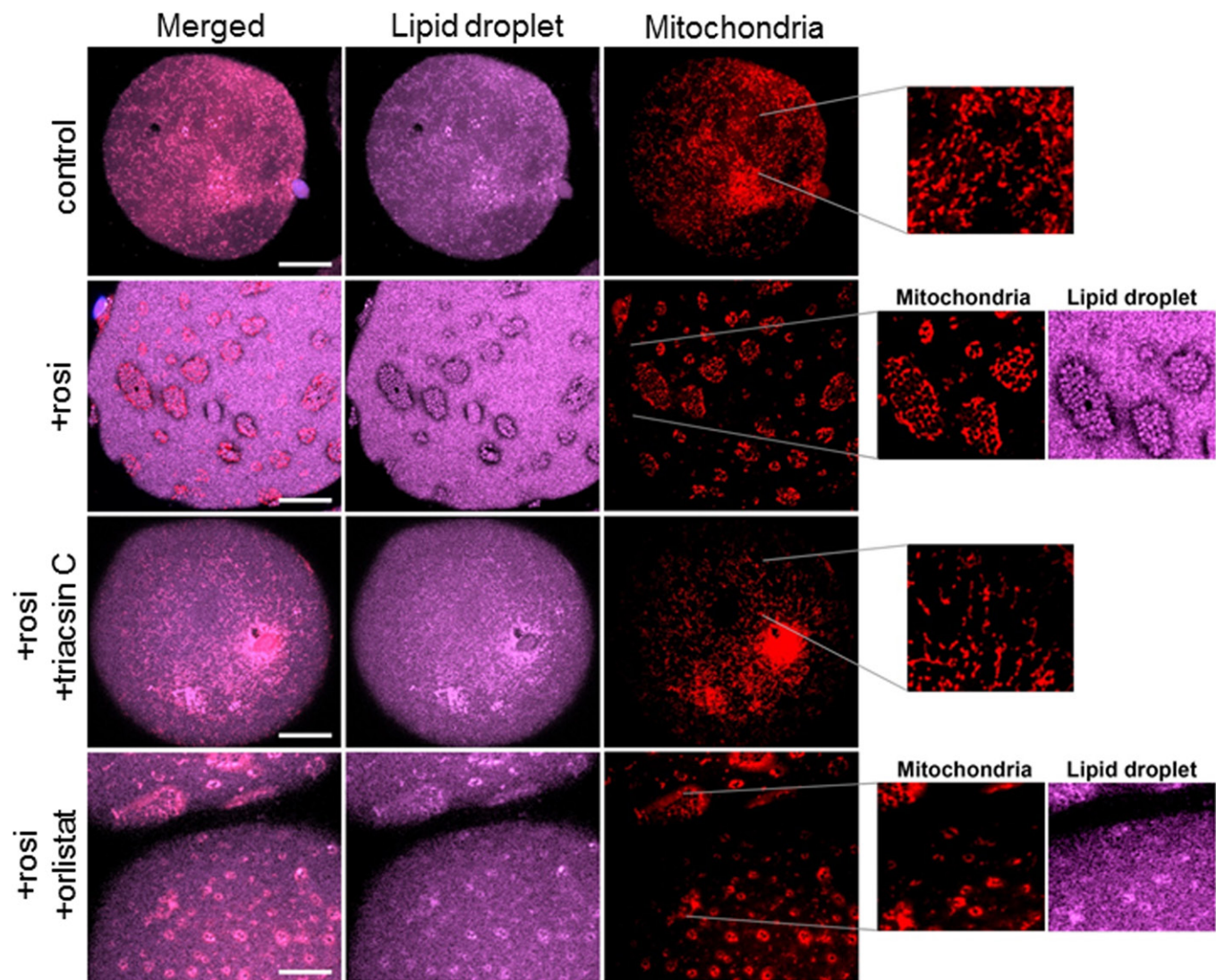
Fig. 5. LD remodeling was blocked by both orlistat and triacsin C while mitochondrial rearrangement was blocked by triacsin C only. After culturing Om adipose tissues with or without Rosi for 5 days, triacsin C or orlistat was added during the final 2 days of culture without or with Rosi, as described in the Materials and Methods. Adipocytes were isolated and stained with LipidTOX-Deep Red and Mitotracker-Red followed by confocal imaging. White scale bars = 10 μm.

Fig. 6. PLIN5 coated the small droplets and colocalized with mitochondria in brite adipocytes. Adipocytes isolated from Om tissues after 7 day culture without or with Rosi were stained with LipidTOX-Deep Red and Mitotracker-Red and used for immunostaining of PLIN1 (A) and PLIN5 (B), as described in the Materials and Methods. White arrows indicate where PLIN5 colocalized with mitochondria. White scale bars = 10 μm.

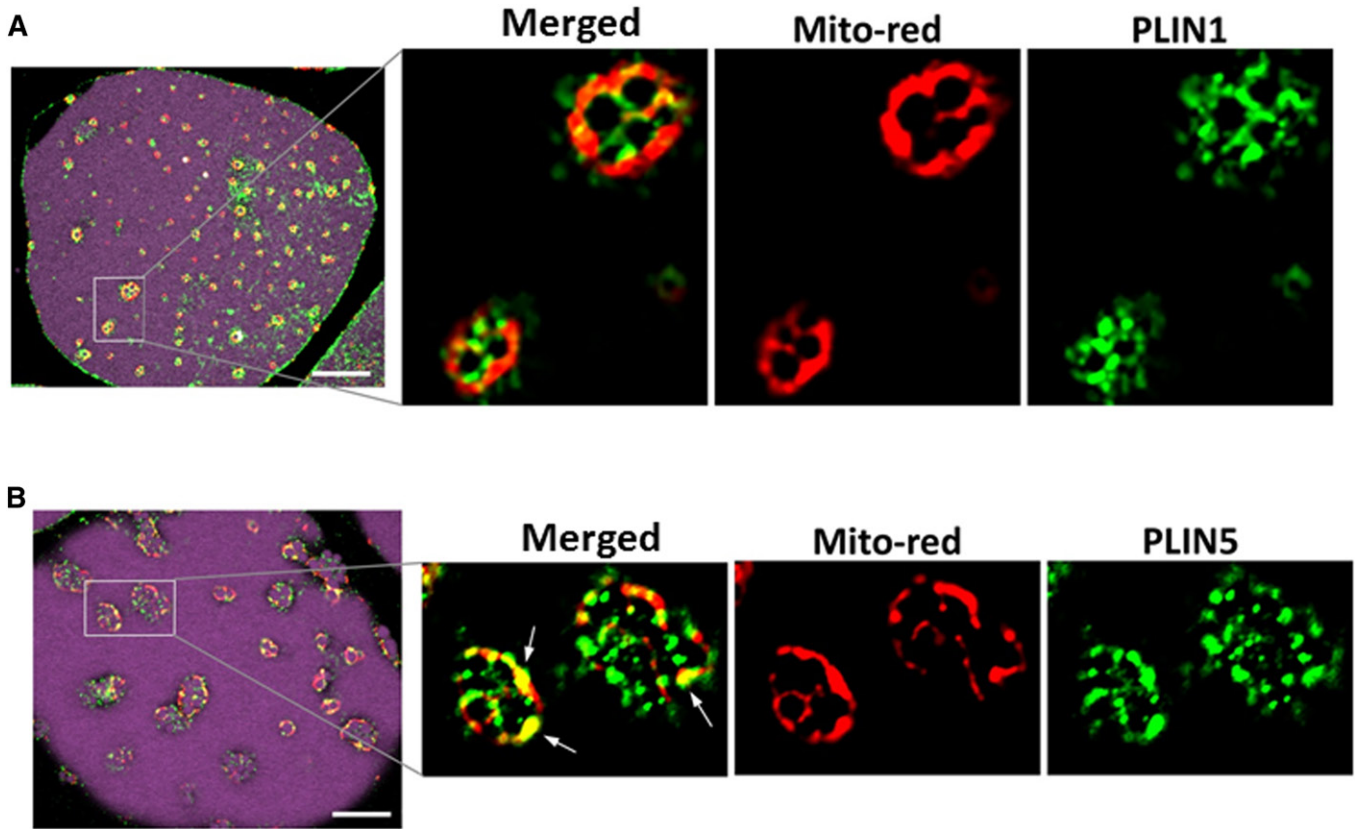Rosi-treated tissue cannot be unambiguously interpreted. We therefore studied primary cultures of human subcutaneous adipocytes. Rosi treatment for 7 days in newly differentiated adipocytes markedly induced the expression levels of UCP1, PLIN5, and FABP3 proteins, similar to the results in adipose tissue organ cultures (**Fig. 7A**). Rosi-treated human adipocytes had higher rates of basal (4.5 ± 0.7-fold) and FCCP-stimulated maximal (4.9 ± 0.5-fold) oxygen consumption and reserve capacity (5.0 ± 0.3-fold) compared with the control (Fig. 7B, C). The higher basal oxygen

consumption was due to a proportional increase in both coupled (ATP-linked) and proton leak, so that coupling efficiency was not different. Furthermore, Rosi did not change the cell respiratory control ratio (ratio of maximal to oligomycin-suppressed rates), indicating that mitochondrial function was not compromised and that sufficient substrate was present to support maximal uncoupled respiration (39).

Because reactive oxygen species (ROS) increase basal leak (44), we treated differentiated adipocytes with Rosi for
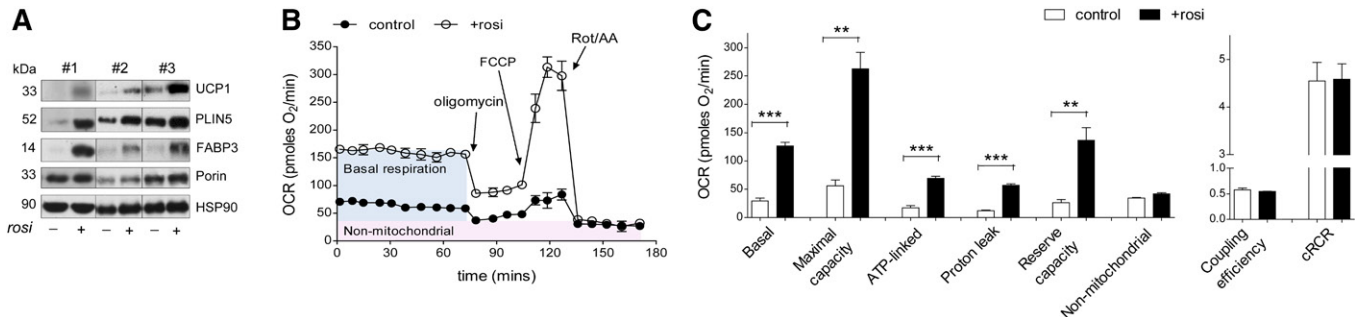
Fig. 7. Rosi increased oxidative capacity in newly differentiated subcutaneous adipocytes. A: Differentiated abdominal subcutaneous adipocytes (day 14) were treated with Rosi for 7 days and protein levels of UCP1, PLIN5, FABP3, and porin were measured. Blots from three different individuals are shown. B: OCRs were measured with a Seahorse extracellular flux analyzer. After measuring basal OCR, the following were injected sequentially: oligomycin (ATP synthase inhibitor), FCCP (uncoupler), and rotenone (complex I inhibitor)/antimycin A (complex III inhibitor) (Rot/AA). The mean ± SD of five wells per condition over time from a representative subject is shown. C: Average values for different components of mitochondrial respiration were calculated (43). Data are expressed as the mean ± SEM of values from three independent subjects (**$P < 0.01$, ***$P < 0.001$ by paired t-tests for Rosi effects).

an additional 7 days, with TNFα (50 pM) added during the final day of culture. Chronic Rosi increased protein carbonylation to the same extent as 24 h TNFα treatment, and the effects were not additive (**Fig. 8**).

Microarray analysis of the Rosi-induced adipose transcriptome

To further interrogate its effects on gene expression globally, we conducted a preliminary analysis of the transcriptome of the Rosi-treated Om adipose tissue from two independent donors. We found upregulation of the KEGG pathways of FA degradation, oxidative phosphorylation, BCAA degradation, FA elongation, ribosome, and peroxisome (supplemental Fig. S2A). Rosi led to an inhibition of inflammatory pathways, including cytokine-cytokine receptor interaction and chemokine signaling (supplemental Fig. S2B). In addition, the most upregulated transcripts included *PM20D1* (3.0- to 4.4-fold), a protein implicated in mitochondrial proton leak (45), and *BBOX1* (2.3- to 3.5-fold), an enzyme responsible for the synthesis of ʟ-carnitine, a molecule needed for FA uptake into mitochondria (supplemental Fig. S2C). Consistent with the anti-inflammatory effects of Rosi, the most downregulated transcripts included *F13A1*, *CCL22*, and *LEP* (supplemental Fig. S2C).

DISCUSSION

We demonstrated that activation of PPARγ with Rosi drove transcriptional changes that reprogrammed metabolism in mature "white" adipocytes from both the Om and subcutaneous human adipose tissues. In both depots, the "britened" adipocytes exhibited higher rates of FA oxidation and increased protein expression of ETC complexes that determine mitochondrial oxidative capacity, as well as UCP1, indicating potential for uncoupled respiration. We

provide evidence that Rosi remodeled the single large LD within white adipocytes so that clusters of SLDs were formed, decorated with PLIN5, and became closely associated with rearranged mitochondria, as illustrated in **Fig. 9**. The similar response in Om and subcutaneous adipocytes is consistent with results from in vivo studies under conditions of high chronic adrenergic activation (14, 15). These coordinated metabolic and structural adaptations may allow the adipocytes of obese individuals to cope with an influx of excess FAs from the diet or high rates of basal lipolysis (2, 3) by efficiently storing them as TAG or oxidizing them, preventing lipotoxicity.

Our results provide insight into the mechanisms that contribute to the formation of the SLDs. The upregulation of mRNAs involved in the synthesis of the glyceride-glycerol backbone of TAG (*GLUT4*, *PCK1*) and (re)esterification (*GPAT3*, *DGAT1*) suggest that the capacity for TAG synthesis is increased, as observed in hMADs (21). Our data showing that inhibition of FA activation or inhibition of lipolysis eliminated the SLDs implicate that they are formed via re-esterification of FAs released from lipolysis of cellular TAG rather than fragmentation of the unilocular LD. De novo synthesis of FAs may also contribute, as we found upregulation of mRNAs for the rate-determining enzymes in the process, *ACC1* and *FAS*. Because inhibition of ACSLs with triacsin C also blocks phospholipid synthesis, it is possible that inhibition of this process might have contributed to the disappearance of the SLDs (46). Further studies would be needed to assess the quantitative importance of these processes to the SLD formation.

We found that Rosi increased lipolysis during culture, as judged by the accumulation of glycerol in culture media. However, rates of lipolysis measured in short-term incubations of isolated adipocytes showed that prior culture with Rosi resulted in lower basal rates of lipolysis. Thus, the higher spontaneous lipolysis in Rosi-treated cultures was
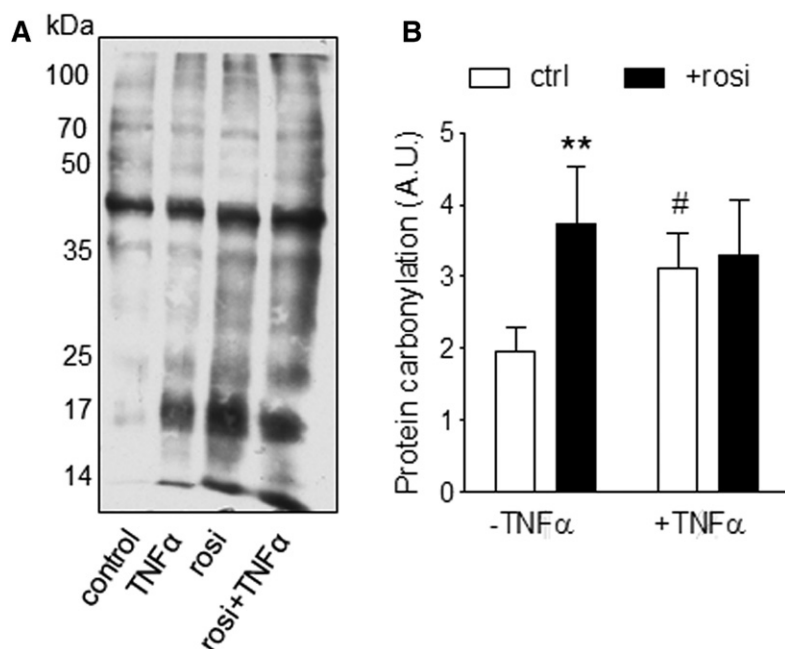
Fig. 8. Rosi increased ROS in human adipocytes. Differentiated abdominal subcutaneous adipocytes were treated with or without Rosi for 7 days with TNFα (50 pM) added during the final 24 h. Protein carbonylation was determined in cell lysates. A representative blot (A) and quantification four independent experiments using cells from different subjects (B) are presented. **Effects of Rosi ($P < 0.01$) and #effects of TNFα ($P < 0.05$) with paired *t*-tests after two-way ANOVA.

Fig. 9. Rosi-mediated metabolic and structural remodeling of human adipocytes. Activation of PPARγ with Rosi drove transcriptional changes that reprogrammed lipid metabolism in mature white adipocytes from both visceral and subcutaneous adipose tissues. The high oxidative capacity in the brite adipocytes was accompanied by a structural remodeling of LDs and mitochondria. Clusters of SLDs were formed, decorated with PLIN5, and became closely associated with rearranged mitochondria. These small droplets were formed through reesterification of FAs released by lipolysis.
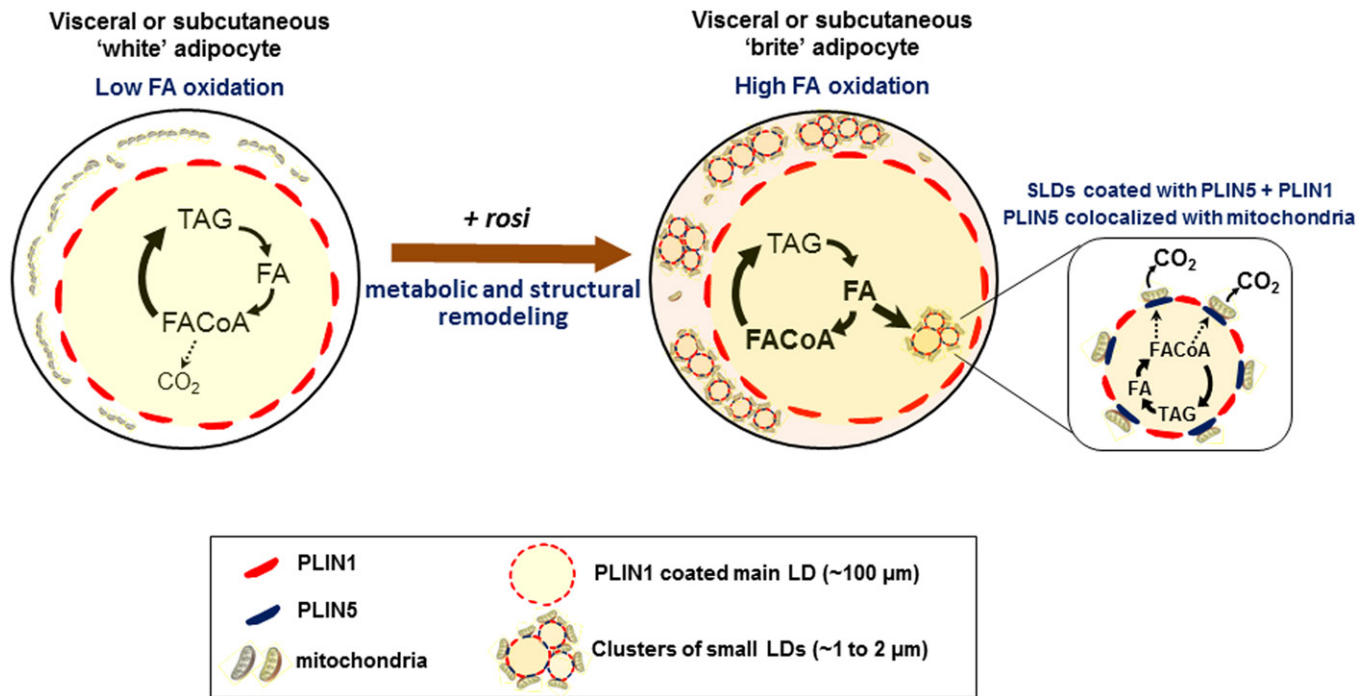
not related to a change in basal lipolytic capacity of the adipocytes and, therefore, was likely a result of changes in local factors under organ culture conditions. Consistent with the lower basal rates in Rosi-britened adipocytes, treatment of type 2 diabetes with thiazolidinediones decreases rates of systemic lipolysis in vivo (47). Adrenergic- and ANP-stimulated lipolysis was similar in control and Rosi-treated adipocytes. However, because of the lower basal rates, the magnitudes of stimulation by adrenergic receptor agonists and ANP were higher in isolated adipocytes from Rosi-treated tissues. The reduction in NPR3, the clearance receptor for ANP (2.0- to 3.5-fold, FDR $q < 0.05$, microarray; supplemental Fig. S2C), may have contributed to the relatively greater ANP effects. This observation is of interest in the context of "britening" because ANP can drive a thermogenic program in cultured human adipocytes (48).

As previously shown in mice (25) and hMADs (21), Rosi increased PLIN5 expression in both Om and ASAT. Further, we found that PLIN5 was closely associated with rearranged mitochondria on SLDs in the brite adipocytes. The functional importance of these findings is not certain. PLIN5 is more highly expressed in oxidative tissues, such as muscle and BAT, where it has been suggested to recruit mitochondria to LDs and enhance FA oxidation (26, 27, 49). Taken together with the evidence that oxidative capacity is increased in the brite adipocytes, our data suggest that PLIN5 may be involved in the recruitment of mitochondria to the SLD surface and stimulation of oxidation of FAs released from lipolysis. The role of PLIN5 to promote FA oxidation in the context of britened adipocytes merits further study.

Studies of cultured brown adipocytes indicated that rates of FA oxidation were lower in mitochondria isolated from the fat cake compared with the cytosolic fraction (50), but it is not known whether similar differences also exist in Rosi-treated white adipocytes. This seems unlikely, as several lines of evidence point to the higher oxidative capacity in mitochondria from Rosi-treated human adipose tissue, including increased cardiolipin content as well as induction of mitochondrial ETC complex proteins and multiple genes in the oxidative phosphorylation pathways. Additional factors may also increase FA oxidation rates in the context of intact brite adipocytes. For example, induction of FABP3 may channel FAs to mitochondria for oxidation, as demonstrated in mouse BAT (41). Furthermore, PLIN5 overexpression does not affect FA oxidation in isolated mitochondria, but increases in homogenates of skeletal muscle containing PLIN5-coated LDs (26). It will be important to compare the oxidative capacity of mitochondria isolated from the fat cake and cytoplasmic fractions to fully understand the mechanisms underlying the higher rates of FA oxidation that we observed in britened mature white adipocytes. Nonetheless, our finding that Rosi induced a more punctate distribution of mitochondria along with increased UCP1 protein is consistent with previous results showing that mitochondrial fission contributes to higher uncoupled respiration in the cultured human adipocyte cell strain, hMADs (51).

We found that culture with Rosi for 7 days increased both basal and maximally stimulated respiration by ∼5-fold in primary cultures of newly differentiated abdominal subcutaneous adipocytes, similar to prior results in hMADs

(51). The higher basal OCR was driven by increases in both ATP-linked and proton leak. Importantly, the Rosi-mediated upregulation of mitochondrial capacity may have been required to meet metabolic demand for ATP production. This demand likely included the ATP needed for FA synthesis and activation for TAG synthesis. The cycle of TAG breakdown and resynthesis consumes ATP and can be considered as a "futile cycle" that is reported to occur in rodent WAT in response to thiazolidinediones (52) or cold exposure (53), providing an adaptive mechanism to fine tune metabolic control (54). These conclusions are restricted to primary cultures of differentiated adipocytes from ASAT. Because Om adipose stem cells exhibit substantially lower rates of adipogenesis (55), it was not possible to compare depot differences in adipocyte OCR measurements.

The higher levels of basal proton leak in Rosi-britened adipocytes could be driven by the increases in UCP1 protein (over 10-fold) as well as mitochondrial anion carrier proteins, including adenine nucleotide translocator (ANT1; ~1.2-fold, FDR q < 0.025) (56). Our microarray study also showed that Rosi upregulated the mRNA expression of PM20D1 (~4-fold, FDR q < 0.001) (45). If this leads to an increased activity of this enzyme, the N-acyl amino acids produced can act as endogenous uncouplers, independent of UCP1, contributing to the higher proton leak observed in Rosi-treated human adipocytes. Additionally, the Rosi-mediated increase in ROS formation, suggested by the observed increase in protein carboxylation, may have also contributed to higher mitochondrial leak (44).

Pioglitazone treatment of obese or type 2 diabetic people increases UCP1 mRNA expression in WAT (18), but does not increase resting metabolic rate, respiratory quotient, or total energy expenditure (57). Thus, we think that the adaptive changes in adipocyte metabolism that we observed in Rosi-treated human adipocytes is unlikely to be important in regulating energy balance or body fat. In contrast, browning of the subcutaneous depot after severe burn injury is associated with increases in resting energy expenditure in humans (15). Induction of UCP1 and other uncouplers by activation of PPARγ could provide a mechanism for higher uncoupled respiration to generate heat rather than ATP when cellular FAs are acutely elevated secondary to sympathetic stimulation or overfeeding (58).

Epididymal fat in C57BL/6 mice is often considered entirely white in that it lacks inducible brite/beige progenitors (28–31) and expresses lower levels of UCP1 than the inguinal subcutaneous depot (59). However, the intraabdominal retroperitoneal and periovarian depots of female 129 Sv mice are browned in response to cold (60). We found that UCP1 protein levels were higher in the Om (visceral) adipose tissue than in the ASAT obtained from mainly female human subjects with a wide range of BMI (29–54 kg/m^2) and cultured under control conditions, similar to previous reports showing higher UCP1 mRNA levels in the Om adipose tissue of humans (59, 61). Furthermore, Rosi increased UCP1 and other brite markers in adipocytes from both depots. The acute responsiveness to lipoytic agonists as well as staining of mitochondria, LDs, and perilipins in adipocytes isolated from tissue after culture confirms that our explant culture system maintains normal morphology and viability of mature adipocytes ex vivo. Given the large size of the "Rosi-britened"adipocytes, they are not derived from beige progenitors that may be present in tissue explants over the time period studied. Rather, they are likely from a metabolic reprogramming of existing mature adipocytes (14, 15). It is tempting to speculate that some of these phenotypically white cells that acquire a "briter" more oxidative phenotype may represent adipocytes with a beige origin that have been "warmed" yet retain the capacity to become metabolically reprogramed (62). While the functional significance of the higher UCP1 expression levels in the visceral depot is unknown, beyond UCP1-mediated thermogenic capacity, other benefits of britening of white adipocytes are recognized (63). The similar responses in Om and ASAT suggest the potential usefulness of novel therapeutic approaches to treat or prevent lipotoxicity in visceral obesity (64, 65).

A limitation of this work is that we only carried out a preliminary analysis of the effects of Rosi on the transcriptome of Om adipose tissue without a direct comparison to ASAT. It is therefore possible that depot differences in sensitivity of mRNAs or pathways to Rosi were missed and it will be important to carry out such studies.

The Rosi-mediated increases in respiration capacity occurred in human adipocytes cultured with a low concentration dexamethasone and insulin. Unlike mice, where dexamethasone whitens brown and brite programs, glucocorticoids enhance thermogenesis and expression of UCP1 genes in human brown adipocytes in vitro (66, 67), and acute administration of glucocorticoids increases metabolic rates in humans in vivo (67). Dexamethasone, added in the presence of insulin, promotes the expression of TAG synthesis enzymes without increasing lipolysis (33, 34), so it may be critical for the upregulation of TAG synthesis and needed for the formation of SLDs and maintenance of brite phenotypes.

In summary, using a PPARγ agonist to probe pathways that could contribute to the britening process, we showed that mature human adipocytes from both visceral and subcutaneous depots can be reprogrammed into brite adipocytes. This transition was associated with coordinated changes in the transcriptome that led to remodeling of LDs and rearrangement of mitochondria as well as enhancement of metabolic capacity. Considering the cardiometabolic side effects of thiazolidinediones, use of partial agonists or developing drugs directed at the downstream targets in FA handling and metabolism identified herein may represent a viable strategy to improve adipocyte and systemic metabolism and prevent or treat obesity-related metabolic diseases.

REFERENCES

1. Gustafson, B., S. Hedjazifar, S. Gogg, A. Hammarstedt, and U. Smith. 2015. Insulin resistance and impaired adipogenesis. *Trends Endocrinol. Metab.* **26:** 193–200.

2. Koutsari, C., and M. D. Jensen. 2006. Free fatty acid metabolism in human obesity. *J. Lipid Res.* **47:** 1643–1650.

3. Rydén, M., and P. Arner. 2017. Subcutaneous adipocyte lipolysis contributes to circulating lipid levels. *Arterioscler. Thromb. Vasc. Biol.* **37:** 1782–1787.

4. Das, S. K., W. S. Chu, A. K. Mondal, N. K. Sharma, P. A. Kern, N. Rasouli, and S. C. Elbein. 2008. Effect of pioglitazone treatment on endoplasmic reticulum stress response in human adipose and in palmitate-induced stress in human liver and adipose cell lines. *Am. J. Physiol. Endocrinol. Metab.* **295:** E393–E400.

5. Frayn, K. N., D. Langin, and F. Karpe. 2008. Fatty acid-induced mitochondrial uncoupling in adipocytes is not a promising target for treatment of insulin resistance unless adipocyte oxidative capacity is increased. *Diabetologia.* **51:** 394–397.

6. Chitraju, C., N. Mejhert, J. T. Haas, L. G. Diaz-Ramirez, C. A. Grueter, J. E. Imbriglio, S. Pinto, S. K. Koliwad, T. C. Walther, and R. V. Farese, Jr. 2017. Triglyceride synthesis by DGAT1 protects adipocytes from lipid-induced ER stress during lipolysis. *Cell Metab.* **26:** 407–418.e3.

7. Bogacka, I., H. Xie, G. A. Bray, and S. R. Smith. 2005. Pioglitazone induces mitochondrial biogenesis in human subcutaneous adipose tissue in vivo. *Diabetes.* **54:** 1392–1399.

8. Cuthbertson, D. J., T. Steele, J. P. Wilding, J. C. Halford, J. A. Harrold, M. Hamer, and F. Karpe. 2017. What have human experimental overfeeding studies taught us about adipose tissue expansion and susceptibility to obesity and metabolic complications? *Int. J. Obes. (Lond.).* **41:** 853–865.

9. Carobbio, S., V. Pellegrinelli, and A. Vidal-Puig. 2017. Adipose tissue function and expandability as determinants of lipotoxicity and the metabolic syndrome. *Adv. Exp. Med. Biol.* **960:** 161–196.

10. Barbatelli, G., I. Murano, L. Madsen, Q. Hao, M. Jimenez, K. Kristiansen, J. P. Giacobino, M. R. De, and S. Cinti. 2010. The emergence of cold-induced brown adipocytes in mouse white fat depots is determined predominantly by white to brown adipocyte transdifferentiation. *Am. J. Physiol. Endocrinol. Metab.* **298:** E1244–E1253.

11. Rosenwald, M., A. Perdikari, T. Rulicke, and C. Wolfrum. 2013. Bi-directional interconversion of brite and white adipocytes. *Nat. Cell Biol.* **15:** 659–667.

12. Seale, P., H. M. Conroe, J. Estall, S. Kajimura, A. Frontini, J. Ishibashi, S. Cohen, S. Cinti, and B. M. Spiegelman. 2011. Prdm16 determines the thermogenic program of subcutaneous white adipose tissue in mice. *J. Clin. Invest.* **121:** 96–105.

13. Wang, Q. A., C. Tao, R. K. Gupta, and P. E. Scherer. 2013. Tracking adipogenesis during white adipose tissue development, expansion and regeneration. *Nat. Med.* **19:** 1338–1344.

14. Frontini, A., A. Vitali, J. Perugini, I. Murano, C. Romiti, D. Ricquier, M. Guerrieri, and S. Cinti. 2013. White-to-brown transdifferentiation of omental adipocytes in patients affected by pheochromocytoma. *Biochim. Biophys. Acta.* **1831:** 950–959.

15. Sidossis, L. S., C. Porter, M. K. Saraf, E. Borsheim, R. S. Radhakrishnan, T. Chao, A. Ali, M. Chondronikola, R. Mlcak, C. C. Finnerty, et al. 2015. Browning of subcutaneous white adipose tissue in humans after severe adrenergic stress. *Cell Metab.* **22:** 219–227.

16. Kern, P. A., B. S. Finlin, B. Zhu, N. Rasouli, R. E. McGehee, Jr., P. M. Westgate, and E. E. Dupont-Versteegden. 2014. The effects of temperature and seasons on subcutaneous white adipose tissue in humans: evidence for thermogenic gene induction. *J. Clin. Endocrinol. Metab.* **99:** E2772–E2779.

17. Rasouli, N., P. A. Kern, S. C. Elbein, N. K. Sharma, and S. K. Das. 2012. Improved insulin sensitivity after treatment with PPARgamma and PPARalpha ligands is mediated by genetically modulated transcripts. *Pharmacogenet. Genomics.* **22:** 484–497.

18. Esterson, Y. B., K. Zhang, S. Koppaka, S. Kehlenbrink, P. Kishore, P. Raghavan, S. R. Maginley, M. Carey, and M. Hawkins. 2013. Insulin sensitizing and anti-inflammatory effects of thiazolidinediones are heightened in obese patients. *J. Investig. Med.* **61:** 1152–1160.

19. Bogacka, I., B. Ukropcova, M. McNeil, J. M. Gimble, and S. R. Smith. 2005. Structural and functional consequences of mitochondrial biogenesis in human adipocytes in vitro. *J. Clin. Endocrinol. Metab.* **90:** 6650–6656.

20. Elabd, C., C. Chiellini, M. Carmona, J. Galitzky, O. Cochet, R. Petersen, L. Penicaud, K. Kristiansen, A. Bouloumie, L. Casteilla, et al. 2009. Human multipotent adipose-derived stem cells differentiate into functional brown adipocytes. *Stem Cells.* **27:** 2753–2760.

21. Barquissau, V., D. Beuzelin, D. F. Pisani, G. E. Beranger, A. Mairal, A. Montagner, B. Roussel, G. Tavernier, M. A. Marques, C. Moro, et al. 2016. White-to-brite conversion in human adipocytes promotes metabolic reprogramming towards fatty acid anabolic and catabolic pathways. *Mol. Metab.* **5:** 352–365.

22. Wilson-Fritch, L., S. Nicoloro, M. Chouinard, M. A. Lazar, P. C. Chui, J. Leszyk, J. Straubhaar, M. P. Czech, and S. Corvera. 2004. Mitochondrial remodeling in adipose tissue associated with obesity and treatment with rosiglitazone. *J. Clin. Invest.* **114:** 1281–1289.

23. Sztalryd, C., and D. L. Brasaemle. 2017. The perilipin family of lipid droplet proteins: Gatekeepers of intracellular lipolysis. *Biochim. Biophys. Acta Mol. Cell Biol. Lipids.* **1862:** 1221–1232.

24. Blanchette-Mackie, E. J., N. K. Dwyer, T. Barber, R. A. Coxey, T. Takeda, C. M. Rondinone, J. L. Theodorakis, A. S. Greenberg, and C. Londos. 1995. Perilipin is located on the surface layer of intracellular lipid droplets in adipocytes. *J. Lipid Res.* **36:** 1211–1226.

25. Wolins, N. E., B. K. Quaynor, J. R. Skinner, A. Tzekov, M. A. Croce, M. C. Gropler, V. Varma, A. Yao-Borengasser, N. Rasouli, P. A. Kern, et al. 2006. OXPAT/PAT-1 is a PPAR-induced lipid droplet protein that promotes fatty acid utilization. *Diabetes.* **55:** 3418–3428.

26. Bosma, M., R. Minnaard, L. M. Sparks, G. Schaart, M. Losen, M. H. de Baets, H. Duimel, S. Kersten, P. E. Bickel, P. Schrauwen, et al. 2012. The lipid droplet coat protein perilipin 5 also localizes to muscle mitochondria. *Histochem. Cell Biol.* **137:** 205–216.

27. Wang, H., U. Sreenevasan, H. Hu, A. Saladino, B. M. Polster, L. M. Lund, D. W. Gong, W. C. Stanley, and C. Sztalryd. 2011. Perilipin 5, a lipid droplet-associated protein, provides physical and metabolic linkage to mitochondria. *J. Lipid Res.* **52:** 2159–2168. [Erratum. 2013. *J. Lipid Res.* 54: 3539.]

28. Guerra, C., R. A. Koza, H. Yamashita, K. Walsh, and L. P. Kozak. 1998. Emergence of brown adipocytes in white fat in mice is under genetic control. Effects on body weight and adiposity. *J. Clin. Invest.* **102:** 412–420.

29. Ohno, H., K. Shinoda, B. M. Spiegelman, and S. Kajimura. 2012. PPARgamma agonists induce a white-to-brown fat conversion through stabilization of PRDM16 protein. *Cell Metab.* **15:** 395–404.

30. Wu, J., P. Bostrom, L. M. Sparks, L. Ye, J. H. Choi, A. H. Giang, M. Khandekar, K. A. Virtanen, P. Nuutila, G. Schaart, et al. 2012. Beige adipocytes are a distinct type of thermogenic fat cell in mouse and human. *Cell.* **150:** 366–376.

31. Shabalina, I. G., N. Petrovic, J. M. de Jong, A. V. Kalinovich, B. Cannon, and J. Nedergaard. 2013. UCP1 in brite/beige adipose tissue mitochondria is functionally thermogenic. *Cell Reports.* **5:** 1196–1203.

32. Vergnes, L., G. R. Davies, J. Y. Lin, M. W. Yeh, M. J. Livhits, A. Harari, M. E. Symonds, H. S. Sacks, and K. Reue. 2016. Adipocyte browning and higher mitochondrial function in periadrenal but not SC fat in pheochromocytoma. *J. Clin. Endocrinol. Metab.* **101:** 4440–4448.

33. Lee, M. J., D. W. Gong, B. F. Burkey, and S. K. Fried. 2011. Pathways regulated by glucocorticoids in omental and subcutaneous human adipose tissues: a microarray study. *Am. J. Physiol. Endocrinol. Metab.* **300:** E571–E580.

34. Lee, M. J., and S. K. Fried. 2012. Glucocorticoids antagonize tumor necrosis factor-alpha-stimulated lipolysis and resistance to the antilipolytic effect of insulin in human adipocytes. *Am. J. Physiol. Endocrinol. Metab.* **303:** E1126–E1133.

35. Frezza, C., S. Cipolat, and L. Scorrano. 2007. Organelle isolation: functional mitochondria from mouse liver, muscle and cultured fibroblasts. *Nat. Protoc.* **2:** 287–295.

36. Laurell, S., and G. Tibbling. 1966. An enzymatic fluorometric micromethod for the determination of glycerol. *Clin. Chim. Acta.* **13:** 317–322.

37. Fried, S. K., T. Tittelbach, J. Blumenthal, U. Sreenivasan, L. Robey, J. Yi, S. Khan, C. Hollender, A. S. Ryan, and A. P. Goldberg. 2010. Resistance to the antilipolytic effect of insulin in adipocytes of African-American compared to Caucasian postmenopausal women. *J. Lipid Res.* **51:** 1193–1200.

38. Lee, M. J., and S. K. Fried. 2014. Optimal protocol for the differentiation and metabolic analysis of human adipose stromal cells. *Methods Enzymol.* **538:** 49–65.

39. Brand, M. D., and D. G. Nicholls. 2011. Assessing mitochondrial dysfunction in cells. *Biochem. J.* **435:** 297–312.

40. Sharp, L. Z., K. Shinoda, H. Ohno, D. W. Scheel, E. Tomoda, L. Ruiz, H. Hu, L. Wang, Z. Pavlova, V. Gilsanz, et al. 2012. Human BAT possesses molecular signatures that resemble beige/brite cells. *PLoS One.* **7:** e49452.

41. Vergnes, L., R. Chin, S. G. Young, and K. Reue. 2011. Heart-type fatty acid-binding protein is essential for efficient brown adipose tissue fatty acid oxidation and cold tolerance. *J. Biol. Chem.* **286:** 380–390.

42. Ikon, N., and R. O. Ryan. 2017. Cardiolipin and mitochondrial cristae organization. *Biochim. Biophys. Acta Biomembr.* **1859:** 1156–1163.

43. Brasaemle, D. L., B. Rubin, I. A. Harten, J. Gruia-Gray, A. R. Kimmel, and C. Londos. 2000. Perilipin A increases triacylglycerol storage by decreasing the rate of triacylglycerol hydrolysis. *J. Biol. Chem.* **275:** 38486–38493.

44. Chouchani, E. T., L. Kazak, and B. M. Spiegelman. 2017. Mitochondrial reactive oxygen species and adipose tissue thermogenesis: bridging physiology and mechanisms. *J. Biol. Chem.* **292:** 16810–16816.

45. Long, J. Z., K. J. Svensson, L. A. Bateman, H. Lin, T. Kamenecka, I. A. Lokurkar, J. Lou, R. R. Rao, M. R. Chang, M. P. Jedrychowski, et al. 2016. The secreted enzyme PM20D1 regulates lipidated amino acid uncouplers of mitochondria. *Cell.* **166:** 424–435.

46. Wang, H., M. V. Airola, and K. Reue. 2017. How lipid droplets "TAG" along: glycerolipid synthetic enzymes and lipid storage. *Biochim. Biophys. Acta Mol. Cell Biol. Lipids.* **1862:** 1131–1145.

47. Boden, G., P. Cheung, M. Mozzoli, and S. K. Fried. 2003. Effect of thiazolidinediones on glucose and fatty acid metabolism in patients with type 2 diabetes. *Metabolism.* **52:** 753–759.

48. Bordicchia, M., D. Liu, E. Z. Amri, G. Ailhaud, P. Dessi-Fulgheri, C. Zhang, N. Takahashi, R. Sarzani, and S. Collins. 2012. Cardiac natriuretic peptides act via p38 MAPK to induce the brown fat thermogenic program in mouse and human adipocytes. *J. Clin. Invest.* **122:** 1022–1036.

49. Laurens, C., V. Bourlier, A. Mairal, K. Louche, P. M. Badin, E. Mouisel, A. Montagner, A. Marette, A. Tremblay, J. S. Weisnagel, et al. 2016. Perilipin 5 fine-tunes lipid oxidation to metabolic demand and protects against lipotoxicity in skeletal muscle. *Sci. Rep.* **6:** 38310.

50. Benador, I. Y., M. Veliova, K. Mahdaviani, A. Petcherski, J. D. Wikstrom, E. A. Assali, R. Acin-Perez, M. Shum, M. F. Oliveira, S. Cinti, et al. 2018. Mitochondria bound to lipid droplets have unique bioenergetics, composition, and dynamics that support lipid droplet expansion. *Cell Metab.* **27:** 869–885.e6.

51. Pisani, D. F., V. Barquissau, J. C. Chambard, D. Beuzelin, R. A. Ghandour, M. Giroud, A. Mairal, S. Pagnotta, S. Cinti, D. Langin, et al. 2018. Mitochondrial fission is associated with UCP1 activity in human brite/beige adipocytes. *Mol. Metab.* **7:** 35–44.

52. Guan, H. P., Y. Li, M. V. Jensen, C. B. Newgard, C. M. Steppan, and M. A. Lazar. 2002. A futile metabolic cycle activated in adipocytes by antidiabetic agents. *Nat. Med.* **8:** 1122–1128.

53. Flachs, P., K. Adamcova, P. Zouhar, C. Marques, P. Janovska, I. Viegas, J. G. Jones, K. Bardova, M. Svobodova, J. Hansikova, et al. 2017. Induction of lipogenesis in white fat during cold exposure in mice: link to lean phenotype. *Int. J. Obes. (Lond.).* **41:** 372–380.

54. Braun, K., J. Oeckl, J. Westermeier, Y. Li, and M. Klingenspor. 2018. Non-adrenergic control of lipolysis and thermogenesis in adipose tissues. *J. Exp. Biol.* **221:** doi:10.1242/jeb.165381.

55. Lee, M. J., R. T. Pickering, V. Shibad, Y. Wu, K. Karastergiou, M. Jager, M. D. Layne, and S. K. Fried. 2019. Impaired glucocorticoid suppression of TGFbeta signaling in human omental adipose tissues limits adipogenesis and may promote fibrosis. *Diabetes.* **68:** 587–597.

56. Shabalina, I. G., T. V. Kramarova, J. Nedergaard, and B. Cannon. 2006. Carboxyatractyloside effects on brown-fat mitochondria imply that the adenine nucleotide translocator isoforms ANT1 and ANT2 may be responsible for basal and fatty-acid-induced uncoupling respectively. *Biochem. J.* **399:** 405–414.

57. Bogacka, I., H. Xie, G. A. Bray, and S. R. Smith. 2004. The effect of pioglitazone on peroxisome proliferator-activated receptor-gamma target genes related to lipid storage in vivo. *Diabetes Care.* **27:** 1660–1667.

58. Li, Y., T. Fromme, and M. Klingenspor. 2017. Meaningful respirometric measurements of UCP1-mediated thermogenesis. *Biochimie.* **134:** 56–61.

59. Zuriaga, M. A., J. J. Fuster, N. Gokce, and K. Walsh. 2017. Humans and mice display opposing patterns of "browning" gene expression in visceral and subcutaneous white adipose tissue depots. *Front. Cardiovasc. Med.* **4:** 27.

60. Giordano, A., A. Smorlesi, A. Frontini, G. Barbatelli, and S. Cinti. 2014. White, brown and pink adipocytes: the extraordinary plasticity of the adipose organ. *Eur. J. Endocrinol.* **170:** R159–R171.

61. Esterbauer, H., H. Oberkofler, Y. M. Liu, D. Breban, E. Hell, F. Krempler, and W. Patsch. 1998. Uncoupling protein-1 mRNA expression in obese human subjects: the role of sequence variations at the uncoupling protein-1 gene locus. *J. Lipid Res.* **39:** 834–844.

62. Roh, H. C., L. T. Y. Tsai, M. Shao, D. Tenen, Y. Shen, M. Kumari, A. Lyubetskaya, C. Jacobs, B. Dawes, R. K. Gupta, et al. 2018. Warming induces significant reprogramming of beige, but not brown, adipocyte cellular identity. *Cell Metab.* **27:** 1121–1137.e5.

63. Sponton, C. H., and S. Kajimura. 2018. Multifaceted roles of beige fat in energy homeostasis beyond UCP1. *Endocrinology.* **159:** 2545–2553.

64. Lee, M. J., Y. Wu, and S. K. Fried. 2013. Adipose tissue heterogeneity: implication of depot differences in adipose tissue for obesity complications. *Mol. Aspects Med.* **34:** 1–11.

65. Tchkonia, T., T. Thomou, Y. Zhu, I. Karagiannides, C. Pothoulakis, M. D. Jensen, and J. L. Kirkland. 2013. Mechanisms and metabolic implications of regional differences among fat depots. *Cell Metab.* **17:** 644–656.

66. Barclay, J. L., H. Agada, C. Jang, M. Ward, N. Wetzig, and K. K. Ho. 2015. Effects of glucocorticoids on human brown adipocytes. *J. Endocrinol.* **224:** 139–147.

67. Ramage, L. E., M. Akyol, A. M. Fletcher, J. Forsythe, M. Nixon, R. N. Carter, E. J. van Beek, N. M. Morton, B. R. Walker, and R. H. Stimson. 2016. Glucocorticoids acutely increase brown adipose tissue activity in humans, revealing species-specific differences in UCP-1 regulation. *Cell Metab.* **24:** 130–141.